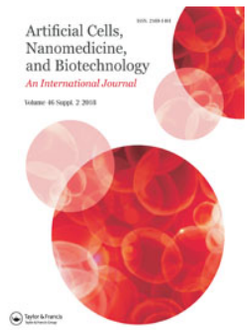

Taylor & Francis
Taylor & Francis Group

Artificial Cells, Nanomedicine, and Biotechnology

An International Journal

ISSN: 2169-1401 (Print) 2169-141X (Online) Journal homepage: https://www.tandfonline.com/loi/ianb20

# Mucoadhesive chitosan-coated PLGA nanoparticles for oral delivery of ferulic acid

Isabela Angeli de Lima, Najeh Maissar Khalil, Tania Toyomi Tominaga, Anna Lechanteur, Bruno Sarmento & Rubiana Mara Mainardes

**To cite this article:** Isabela Angeli de Lima, Najeh Maissar Khalil, Tania Toyomi Tominaga, Anna Lechanteur, Bruno Sarmento & Rubiana Mara Mainardes (2018) Mucoadhesive chitosan-coated PLGA nanoparticles for oral delivery of ferulic acid, Artificial Cells, Nanomedicine, and Biotechnology, 46:sup2, 993-1002, DOI: 10.1080/21691401.2018.1477788

**To link to this article:** https://doi.org/10.1080/21691401.2018.1477788

ARTIFICIAL CELLS, NANOMEDICINE, AND BIOTECHNOLOGY
2018, VOL. 46, NO. S2, S993–S1002
https://doi.org/10.1080/21691401.2018.1477788



# Mucoadhesive chitosan-coated PLGA nanoparticles for oral delivery of ferulic acid

Isabela Angeli de Lima[a], Najeh Maissar Khalil[a], Tania Toyomi Tominaga[b], Anna Lechanteur[c,d], Bruno Sarmento[c,e,f] and Rubiana Mara Mainardes[a]

[a]Department of Pharmacy, Laboratory of Pharmaceutical Nanotechnology, Universidade Estadual do Centro-Oeste/UNICENTRO, Guarapuava, Brazil; [b]Department of Physics, Universidade Estadual do Centro-Oeste/UNICENTRO, Guarapuava, PR, Brazil; [c]INEB – Instituto de Engenharia Biomédica, Universidade do Porto, Porto, Portugal; [d]Laboratory of Pharmaceutical Technology and Biopharmacy (LPTB) CIRM, Department of Pharmacy, University of Liege, Liege, Belgium; [e]i3S – Instituto de Investigação and Inovação em Saúde, Universidade do Porto, Porto, Portugal; [f]CESPU – Instituto de Investigação e Formação Avançada em Ciências and Tecnologias da Saúde, Gandra, Portugal

**ABSTRACT**

This paper describes the development and *in vitro* evaluation of poly(lactic-co-glycolic acid) (PLGA) nanoparticles coated with chitosan (CS) for oral delivery of ferulic acid (FA). Nanoparticles were obtained by an emulsion evaporation technique and characterized. Furthermore, we evaluated the scavenging activity over hypochlorous acid (HOCl), the cytotoxicity over tumour cells and the *in vitro* intestinal permeability. Nanoparticles were spherical with a mean diameter of 242 nm, positive zeta potential and 50% of encapsulation efficiency. The *in vitro* release in phosphate buffered saline (PBS) (pH 7.4) demonstrated a prolonged and biphasic profile diffusion-controlled. In simulated gastrointestinal fluids, about 15% of FA was released in gastric fluid and a negligible release was observed in the intestinal fluid. In the HOCl scavenging activity and cytotoxicity over B16-F10 and HeLa cells, FA-loaded nanoparticles presented the same efficacy of the free drug. Besides, in the antioxidant and cytotoxic assay, CS contributed to FA effects. In the intestinal permeability study, FA-loaded nanoparticles exhibited a permeation of 6% through the Caco-2 monolayer and 20% through the Caco-2/HT29-MTX/Raji B co-culture. CS-coated PLGA nanoparticles are promising carriers for oral delivery of FA.

**ARTICLE HISTORY**
Received 11 January 2018
Revised 7 May 2018
Accepted 8 May 2018

**KEYWORDS**
Artificial cells; Caco-2 cells; chitosan; ferulic acid; HOCl; intestinal permeability; nanoparticles

## Introduction

Ferulic acid (FA) is a polyphenol present in fruits, vegetables and some beverages (such as coffee and beer), which has high antioxidant activity, acting as a free radical scavenger [1]. Its antioxidant action is due to its unsaturated side chain and to the phenolic nucleus, which allows the spontaneous stabilization of structures by resonance. Furthermore, studies have shown that FA presents antitumour, anti-inflammatory, hepatoprotective, vasodilatory, antithrombotic, antiallergic, antiviral, antimicrobial and photoprotective activity. Most of these pharmacological effects are results of the antioxidant activity of FA [2]. It is well known for the role of reactive oxygen species (ROS) in lipid peroxidation, enzyme oxidation and massive protein degradation and oxidation. Effects as cell degradation, DNA damage and carcinogenesis can be caused by excessive ROS and they can trigger a variety of diseases and disorders, such as aging, cancer, hypertension, cardiac and neurodegenerative diseases, rheumatoid arthritis, diabetes mellitus and atherosclerosis [3]. Thus, the study and search for antioxidants that can restrain radicals and slow the progress of chronic diseases are essential [4]. However, the potential of FA, due to its low solubility and permeability, FA absorption from the gastrointestinal tract (GIT) is limited when administered by conventional oral dosage forms, such as tablets and granules, hindering its efficacy [5]. Some micro and nanotechnological approaches have been done to improve the physicochemical, biopharmaceutical and pharmacokinetic of FA, thus increasing its bioavailability [5–8].

The application of nanoparticles in drug delivery is an important tool to circumvent physicochemical and biopharmaceutical drug drawbacks and improve drug bioavailability. Nanoparticles can permeate interstitial spaces enhancing the cellular uptake of the drug [9].

Poly(lactic-co-glycolic acid) (PLGA) is a copolymer widely used as a matrix for nanoparticles due to its biocompatible and biodegradable characteristics [10]. Chitosan (CS) is a natural, biodegradable and biocompatible polysaccharide derived from total or partial deacetylation of chitin [11]. Its mucoadhesive property, when positively charged, allows the interaction with negatively charged membranes and mucosa, promoting a greater interaction, adhesion and retention of the pharmaceutical form-containing CS close to the intestinal epithelium [12]. In addition, CS has the ability to temporarily open the tight junctions of the intestinal epithelium, thereby increasing the drug permeability [13].

In this work, PLGA nanoparticles coated with CS containing FA for oral delivery were developed, characterized and

CONTACT Rubiana Mara Mainardes rubianamainardes@hotmail.com Departamento de Farmácia, Laboratório de Nanotecnologia Farmacêutica, Universidade Estadual do Centro-Oeste – UNICENTRO, Rua Simeão Camargo Varela de Sá, 03 - 85040-080 – Guarapuava – PR, Brazil

*in vitro* evaluated for the antioxidant activity, cytotoxicity over tumour cells lines (B16-F10 and HeLa). Also, the nanoparticles permeability through Caco-2 monolayer and Caco-2/HT29-MTX/Raji B co-culture was carried out.

## Materials and methods

### Materials and reagents

3,3′,5,5′-Tetramethylbenzidine (TMB), ferulic acid (FA; 99%), 3-(4,5-Dimethylthiazol-2-yl)-2,5-diphenyltetrazolium bromide (MTT), glucose, Dulbecco's modified Iscove's medium, pancreatin of porcine pancreas (P1625), porcine gastric mucosal pepsin (P7125), polyvinyl alcohol (PVA; 31 KDa, 88% hydrolysed), poly(lactic-co-glycolic acid) (PLGA; 65:35, 40000–75000 Da) and chitosan (CS; Medium molecular weight, 75–85% deacetylated) were purchased from Sigma-Aldrich (St. Louis, MO). Isopropyl alcohol, dichloromethane and ethanol (95%) were purchased from Fmaia (Cotia, Brazil). Sodium chloride, dibasic sodium phosphate, sodium hydroxide and hydrogen peroxide (30%) were purchased from Biotec (São Paulo, Brazil). HPLC grade acetonitrile was obtained from LiChrosolv-Merck (Darmstadt, Germany). Sodium heparin was purchased from Hipolabor (Sabará, Brazil). Hank's Balanced Salt Solution (HBSS) and tripsin were purchased from Gibco (Carlsbad, CA). Streptomycin and penicillin were purchased from Sigma Aldrich (St. Louis, MO) and Invitrogen Corporation (Life Technologies, S.A., Madrid, Spain). Fetal bovine serum was obtained from Gibco. Non-essential amino acids (NEAA) were purchased from Invitrogen Corporation (Life Technologies, S.A., Madrid, Spain). Triton X-100 was purchased from Spi-Chem (West Chester, PA). Dulbecco's modified Eagle medium was obtained from Lonza (Verviers, Belgium). B16-F10, HeLa, C2BBe1 clone of Caco-2 was obtained from American Type Culture Collection (ATCC, Manassas, VA), HT29-MTX and Raji B were provided by Dr. T. Lesuffleur (INSERMU178, Villejuif, France) and by Dr. Alexandre Carmo (Cellular and Molecular Biology Institute – IBMC, Porto, Portugal), respectively.

### Preparation of chitosan-coated poly(lactic-co-glycolic acid) nanoparticles containing ferulic acid (NP-PLGA-CS-FA)

NP-PLGA-CS-FA was obtained by a single-emulsion solvent evaporation technique, according to a methodology proposed by our group [14], with some modifications. Initially, 50 mg of PLGA and 10 mg of FA were dissolved in 2 mL of a mixture of ethanol and dichloromethane, compounding the organic phase. The aqueous phase consisted of 10 mL of CS solution (0.16%, w/v) and polyvinyl alcohol (PVA, 1%, w/v), both prepared in 2% acetic acid (v/v). The organic phase was then poured into the aqueous phase, and sonicated for 5 min (ultrasonic probe QR1000, Eco-Sonic, Indaiatuba, SP, Brazil) to obtain an oil-in-water emulsion. Subsequently, the organic solvent was evaporated in a rotatory evaporator (TE 120 – Tecnal, Piracicaba, SP, Brazil) under vacuum at 37 °C (15 min). The nanoparticles were recovered by ultracentrifugation (20,635 *g*, 20 °C, 45 min; Z36HK Centrifuge, Hermle Wehingen, BH, Germany) and suspended in cryoprotectant sucrose (15%; w/v). After, the resulting suspension was frozen at –18 °C and lyophilized (Terroni, Brazil). Unloaded nanoparticles (blank) (NP-B) were similarly obtained, but without FA.

### Physicochemical characterization of chitosan-coated poly(lactic-co-glycolic acid) nanoparticles containing ferulic acid (NP-PLGA-CS-FA)

The determination of the mean diameter and the polydispersity index (PDI) was performed by Dynamic Light Scattering (DLS) (BIC 90 plus, Brookhaven Instruments Corp., Holtsville, NY).

The zeta potential of nanoparticles was determined by the Laser Doppler Anemometry, based on the electrophoretic mobility (Zetasizer ZS, Malvern, UK).

The morphology of nanoparticles was examined by scanning electronmicroscopy equipped with a field emission gun (FEG-SEM) (MIRA3 LM, Tescan, Czech Republic).

The percentage of encapsulation efficiency (%EE) was performed indirectly. After the nanoparticles ultracentrifugation, the supernatant containing non-entrapped FA was analysed by HPLC, according to our previously validated methodology [15], using a Waters 2695 Alliance HPLC (Waters Corporation, Milford, MA). The %EE was determined for at least three replicates, according to Equation (1).

$$\%EE = (\text{initial drug amount} \times \text{recovered drug} / \text{initial drug amount}) \times 100 \quad (1)$$

### *In vitro* FA release assay in simulated gastric fluid, simulated intestinal fluid and phosphate buffered saline pH 7.4

Nanoparticles containing about 80 μg of FA were dispersed in 1 mL of simulated gastric fluid (SGF – 50 mM KCl, pH 1.2) and stirred in an orbital shaker (150 rpm, 37 °C). After predetermined times (0.5, 1 and 2 h), the suspensions were centrifuged (20,635*g*, 20 °C, 15 min) and the supernatant was collected for further HPLC analysis. The precipitate was resuspended in the same amount of fresh medium and nanoparticles returned to stirring. After centrifugation and collection of the supernatant in 2 h, the precipitate was suspended in 1 mL of simulated intestinal fluid (SIF – 50 mM $KH_2PO_4$, 15 mM NaOH, 1.0% (w/v) pancreatin; pH 6.5) and agitated for further 4 h, with sampling intervals and replacement of intestinal medium at 3, 4, 5 and 6 h (relative to total test time). The assay was performed under sink conditions.

Release assay was also performed in phosphate buffered saline (PBS, 50 mM, pH 7.4) containing tween 80 (1%, m/v). Nanoparticles containing about 80 μg of FA were dispersed in 1 mL PBS and stirred for a total period of 120 h. The ultracentrifugation and sampling of the supernatants occurred in the periods of 0.5; 2; 4; 8; 24; 48; 72, 96 and 120 h. The release profile data were analysed by mathematical studies according to zero order, first order, second order, Higuchi and Korsmeyer–Peppas models [16].

### *Hypochlorous acid (HOCl) scavenging assay*

The antioxidant activity of nanoparticles was evaluated by the hypochlorous acid (HOCl) inhibition, which was prepared immediately before use, from sodium hypochlorite solution and basified water (pH 12.0). HOCl concentration was verified spectrophotometrically at 292 nm ($\varepsilon_{292nm} = 350\ M^{-1}\ cm^{-1}$). Samples of free FA, NP-PLGA-CS-FA (0.5, 1.0, 2.0 and 2.5 μg/mL FA) and NP-B, diluted in phosphate buffer (50 mM, pH 7.4) and incubated at 37 °C and 150 rpm at periods of 0, 24, 48 and 96 h, were added to the HOCl (50 μM). After 15 min, 20 μL of 10 mmol/L 3,3',5,5'-tetramethylbenzidine solution (TMB) was added, dissolved in 50% dimethylformamide, potassium iodide (100 mmol/L) and acetic acid (400 mmol/L). Then, after 5 min, the absorbance was measured at 650 nm in a microplate reader (Spectra Max 190, Molecular Devices, Sunnyvale, CA). The solution of phosphate buffer was considered as control. The assay was performed in triplicate. The antioxidant activity was determined as a percentage of inhibition, according to Equation (2):

$$\%\ Inhibition = (Abs\ control - Abs\ test / Abs\ control) \times 100 \quad (2)$$

### *Cytotoxicity assays*

#### *Cell culture*

B16-F10 (ATCC CRL-6475) and HeLa (ATCC CCL-2) were cultured in Iscove's modified Dulbecco's medium supplemented with penicillin (10,000 U/mL), streptomycin (10 mg/mL) and 10% (v/v) of fetal bovine serum. Cells used in the intestinal permeability study, Caco-2, HT29-MTX and Raji B, were cultured in Dulbecco's modified Eagle medium (DMEM) and supplemented with 10% (v/v) of fetal bovine serum, 1% (v/v) penicillin (100 U/mL), streptomycin (100 μg/mL) and 1% (v/v) non-essential amino acids (NEAA). All cells were maintained in a water-saturated atmosphere, at 37 °C and 5% $CO_2$.

#### *Cytotoxicity over HeLa and B16-F10 tumour cells lines*

The cytotoxicity of the nanoparticles was evaluated by the MTT quantitative colorimetric method, in tumour cells of melanoma (B16-F10) and cervical cancer cells (HeLa). Initially, cells were seeded in 96-well plates ($1 \times 10^5$ cells/mL) and incubated for 24 h at 37 °C and 5% $CO_2$. After the medium was removed and the cells were exposed to free FA or NP-PLGA-CS-FA at final concentrations of 5, 10, 30 and 60 μg/mL of FA. Controls containing Iscove medium, solvent (ethanol) and NP-B were also tested. After 24 and 48 h, cells were washed with PBS (pH 7.4) and the MTT was added to the wells and the plate was incubated for 3 h (37 °C and 5% $CO_2$). After, MTT medium was removed and 50 μL of ethanol and 150 μL of a mixture PBS (pH 7.4) with isopropyl alcohol (1:1) were added. The absorbance of each well was read on a microplate reader (Spectra Max 190, Molecular Devices, Sunnyvale, CA) at 570 nm. The experiments were performed in triplicate and the cell viability was determined by Equation (3):

$$Cell\ viability\ (\%) = (Abs\ samples / Abs\ control) \times 100 \quad (3)$$

### *In vitro* intestinal permeability assay

The intestinal permeability was determined based on the works of Antunes et al. [17] and Araújo et al. [18]. Monocultures of Caco-2 cells and a triple co-culture of Caco-2:HT29-MTX:Raji B (in a ratio of 90:10 between Caco-2 and HT29-MTX cells) were grown in 6-well Transwell TM plates (pore diameter 3 μm, polycarbonate, 4.67 $cm^2$) (Corning Life Sciences, Amsterdam, The Netherlands). Caco-2 and HT29-MTX cells were seeded in Transwell cell culture inserts at final concentration of $1 \times 10^5$ cells/$cm^2$ and incubated for 14 days, with medium replacement every 2 days. Subsequently, in order to induce the phenotype change of Caco-2 cells in M cells and produce a triple model co-culture, Raji B cells were added to the basolateral chamber, at a concentration of $1 \times 10^5$ cells/$cm^2$, and were incubated for more 7 days.

Then, in orbital shaking incubator (IKA KS 4000 IC Control, Germany) at 37 °C and 100 rpm, the permeability experiments were performed in triplicate in the apical to basolateral direction in Hank's balanced salt solution (HBSS) buffer. The initial apical concentration of FA-loaded nanoparticles was 300 μg/mL in a final volume of 1.5 mL. At predetermined times of 15, 30, 60, 120 and 180 min, samples (200 μL) were collected from the basolateral compartment and the same amount of fresh HBSS (pH 7.4) buffer was added, to replace the withdrawn volume. The quantification of FA in the collected samples was performed by HPLC and the integrity of the cell monolayers was evaluated by the measurement of the transepithelial electrical resistance (TEER) before, during and at the end of permeability assay, using an EVOM epithelial voltohmmeter equipped with chopstick electrodes (World Precision Instruments, Sarasota, FL) [13]. The results were expressed as permeability and TEER percentage.

### *Statistical analysis*

Data were expressed as mean ± standard deviations. One-way analysis of variance (ANOVA) was used for the characterization and cytotoxicity of Caco-2 cells data. For the antioxidant and the cytotoxicity assay over B16-F10 and HeLa tumour cells line, two-way ANOVA was used. Both with Tukey post-test for multiple comparisons of values. For the intestinal permeability assay, the analysis was realized by two-way ANOVA with Sidak post-test. Differences were considered significant if $p < .05$.

## Results and discussion

### *Preparation and characterization of NP-PLGA-CS-FA*

NP-PLGA-CS-FA were efficiently obtained by the single-emulsion solvent evaporation method, a very efficient method for encapsulating a wide variety of hydrophobic compounds. The main physicochemical characteristics of nanoparticles are shown in Table 1. It was found that the drug incorporation into the nanoparticles did not alter the mean diameter and PDI ($p > .05$), however, the addition of CS led to an increase in these parameters ($p < .05$). It may be explained due to CS-related viscosity increase, which reduces the shear stress

**Table 1.** Mean diameter, polydispersity index, zeta potential and encapsulation efficiency of FA-loaded chitosan coated PLGA nanoparticles (NP-PLGA-CS-FA), blank nanoparticles (NP-B) and FA-loaded PLGA nanoparticles without chitosan coating (NP-PLGA-FA).

| Formulation | Mean diameter (nm) | Polydispersity index | Zeta potential (mV) | Encapsulation efficiency ± (%) |
|---|---|---|---|---|
| NP-PLGA-CS-FA ($n = 10$) | $242 \pm 19^{a}$ | $0.20 \pm 0.03^{a}$ | $+32 \pm 5^{a}$ | $50 \pm 4^{a}$ |
| NP-B ($n = 3$) | $248 \pm 14^{a}$ | $0.23 \pm 0.07^{a}$ | $+32 \pm 7^{a}$ | NA |
| NP-PLGA-FA ($n = 3$) | $196 \pm 4^{b}$ | $0.11 \pm 0.02^{b}$ | $-10 \pm 1^{b}$ | $60 \pm 3^{b}$ |

NA: not applicable.

[a,b]Values are reported as mean diameter, polydispersity index, zeta potential and encapsulation efficiency ± standard deviation per column analysed. Same letters mean statistical equality and inequality statistics are shown for different letters (One way-ANOVA with post-Tukey test and $\alpha = 0.05$).

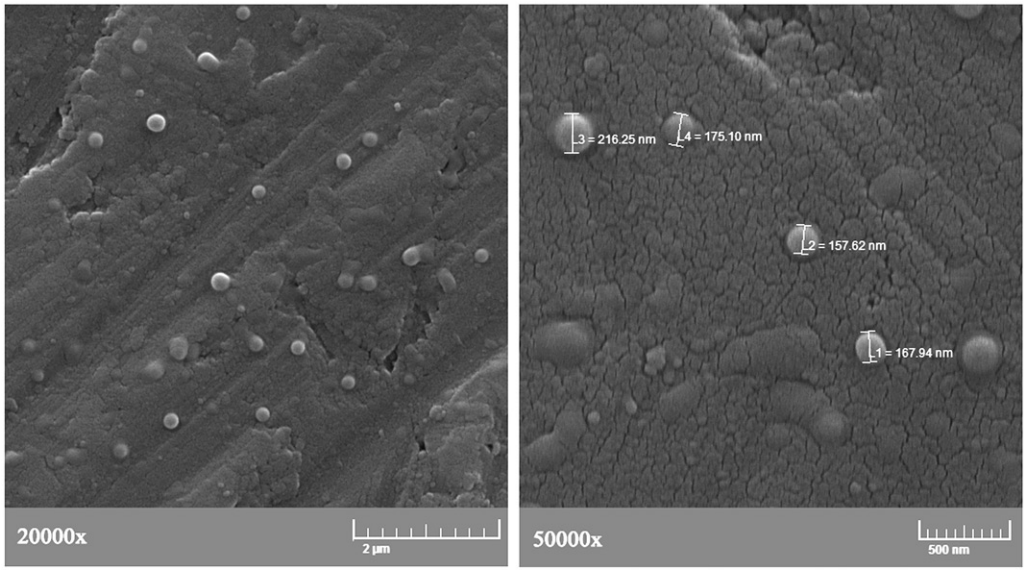


**Figure 1.** FEG-SEM micrographs of PLGA-CS-FA nanoparticles. Magnification of 20 kx and 50 kx.

during sonication of the emulsion, and then leads to an increase in the size of the emulsion droplets [19]. Similar results were obtained by Nafee et al. [20], which obtained CS-modified PLGA nanoparticles and by Yuan et al. [21], which developed PLGA-CS nanoparticles as siRNA carriers. The mean diameter of NP-PLGA-CS-FA was about 250 nm and PDI was 0.2. For the oral administration of polymeric nanoparticles, the particle size below 300 nm is desirable since the particles are able to reach microcirculation by the blood capillaries or penetrate through pores present in the surfaces and membranes [22]. PDI value demonstrated a homogeneous distribution of particle sizes, since a PDI between 0.1 and 0.25 indicates a narrow distribution range. Also, NP-PLGA-CS-FA presented a spherical or slightly oval morphology, without agglomerates, as showed in Figure 1.

PLGA in neutral medium has negative surface potential, attributed to the terminal carboxyl groups [23], and this could be verified by the zeta potential of –10 mV obtained in uncoated PLGA nanoparticles. However, when the CS coating was added, the zeta potential of the particles increased significantly to +32 mV ($p < .05$). This is a consequence of the amino groups present in this polysaccharide and suggests that the PLGA-FA nanoparticles were adequately coated by CS. Besides the high stability promoted by this high modulus value, positive surface charges are attracted by the negatively charged cell membranes, promoting adhesion and retention of the system at the site of action and in the intestinal epithelium, as well as increasing the absorption of the nanometric system [12]. The adherence to cancer cells is also increased since most tumour cells have negatively charged membranes [24]. In addition, the presence of CS may decrease the absorption and interaction of nanoparticles by phagocytes; because this absorption occurs more frequently on hydrophobic and negatively charged surfaces [25].

The encapsulation efficiency of FA in CS-coated PLGA nanoparticles was about 50%. The addition of the coating also interfered with this parameter ($p < .05$), slightly decreasing the amount of encapsulated drug. Parveen and Sahoo [25], also observed this phenomenon when PLGA nanoparticles containing paclitaxel were coated with CS and presented as a probable cause the CS hydrophilicity, which could prevent the entrapment of the hydrophobic drug.

## *In vitro* FA release assay in simulated gastric fluid, simulated intestinal fluid and phosphate buffered saline pH 7.4

In order to predict the FA release in GIT similar conditions, nanoparticles were incubated for 2 h in SGF (pH 1.2) and after 2 h the same nanoparticles were incubated in SIF (pH 6.5), remaining 4 h in this medium. The results are shown in Figure 2(A). When added to SGF, CS-coated PLGA nanoparticles released only about 15% of FA after 2 h-incubation. This release may be due to the FA adsorbed on the nanoparticles

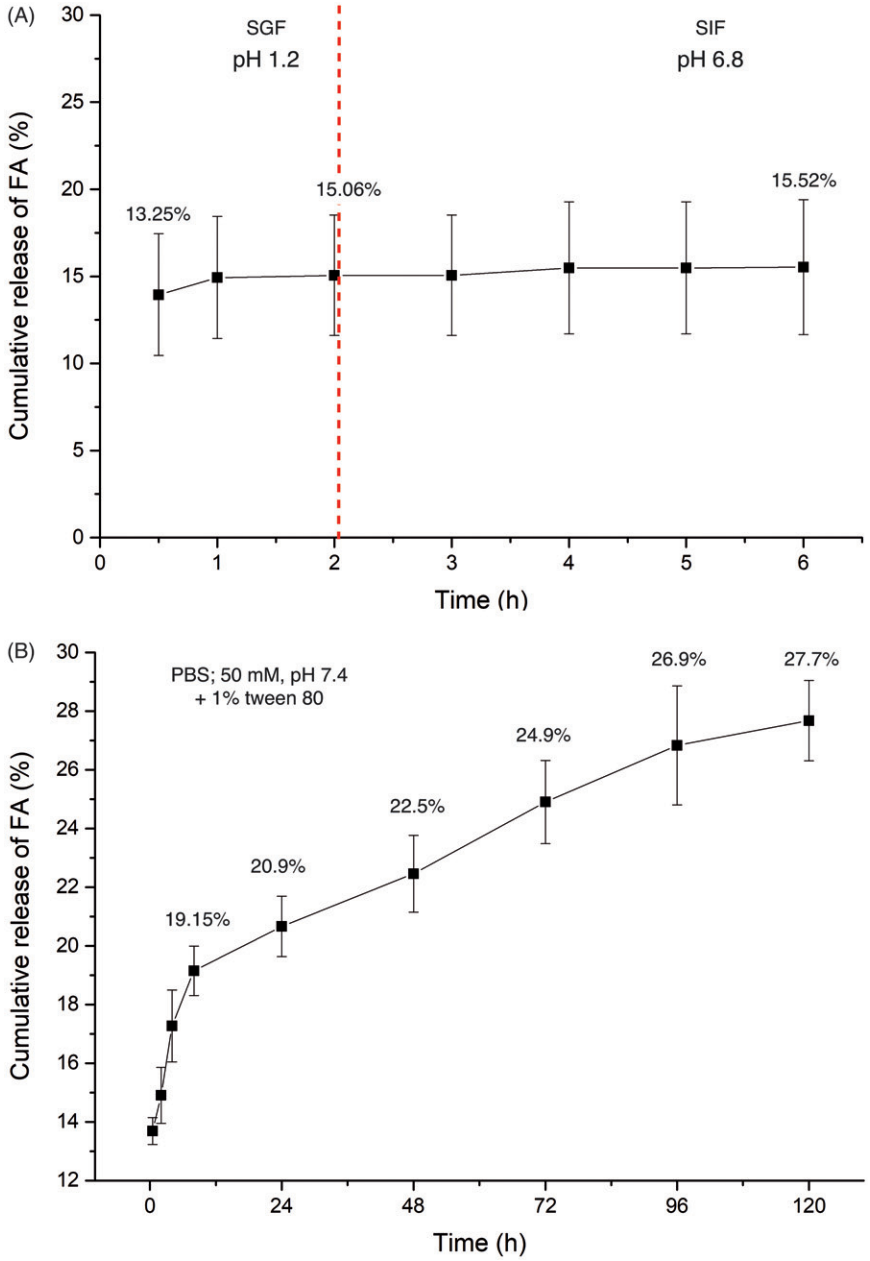


**Figure 2.** Release profile of FA from PLGA-CS nanoparticles in: (A) simulated gastric (SGF; pH 1.2) and intestinal (SIF; pH 6.8) fluids. The assay was conducted for 2 h in SGF and for 4 h in SIF. (B) Phosphate buffered saline (PBS; 50 mM, pH 7.4) containing tween 80 (1%). Results were expressed as mean ± standard deviation ($n = 3$).

surface, which is rapidly released due to weak interactions between the drug and polymer, characterizing a burst effect. After changing the medium to SIF, only 0.5% of FA was released from nanoparticles, after 4 h-incubation. The higher FA release in the acid medium may also be due to the higher CS solubility at low pHs. In acidic media, the CS amine groups are mostly protonated leading to the CS dissolution in the aqueous medium, decreasing the coating layers that surround the nanoparticles, and thus allowing an increase in drug diffusion by the PLGA matrix [12]. At the end of the assay, about 15.5% of the encapsulated FA was released into the medium. These results suggest the potential use of PLGA-CS nanoparticles in the FA oral administration, since nanoparticles could efficiently retain most part of drug content under GIT conditions. Thus, FA-loaded PLGA-CS nanoparticles may be absorbed by the intestinal cells, leading to an improved FA bioavailability.

The FA release profile from NP-PLGA-CS in PBS (50 mM, pH 7.4) can be seen in Figure 2(B). A biphasic release profile was obtained, characterized by a fast release followed by a sustained release. An initial drug release occurred, in which 19.15% of total FA was released in 8 h. This initial phenomenon is characterized by the detachment of the drug adsorbed on the nanoparticles surface, which is weakly bound to the polymer. After, there was a slower and prolonged release, characteristic of polymeric nanoparticles and it is due to the drug diffusion from the polymeric matrix. After 120 h, about 28% of FA was released from the nanoparticles. Similar results were obtained by other authors. Chronopoulou et al. [12] showed a very slow and sustained

release of dexamethasone from PLGA-CS nanoparticles. They attributed this characteristic to a strong interaction between the drug and CS, and also to the coating property in acting as a physical barrier to the drug diffusion. Parveen and Sahoo [25] showed after 120 h of assay about 20% of paclitaxel was released from CS-coated PLGA nanoparticles. It also has been found that the addition of CS decreased the release rate of paclitaxel. It can be assumed that the release of FA from PLGA-CS nanoparticles did not present high values due to the same principle of matrix protection by the CS coating, leading to a lower diffusion of the drug.

The kinetic modelling obtained from the release data in PBS revealed that the FA release from nanoparticles followed the second-order model, i.e. the release is guided by two release constants or kinetic constants, α and β. The constant α is responsible for the rapid stage of release, related to release of the drug located more externally in the nanoparticle. And the β constant is related to the slow step, resulting from the dissolution of the drug located more internally. For the Korsmeyer–Peppas model, used to predict the mechanism of drug or compound release, an *n* of 0.1344 was found, indicating that the FA release process was regulated by the diffusion process through the polymeric matrix [16,26].

Table 2. Percentage of hypochlorous acid (HOCl) inhibition by free ferulic acid (FA), FA-loaded chitosan-coated PLGA nanoparticles (NP-PLGA-CS-FA) and blank nanoparticles (NP-B), in 0, 24, 48 and 96 h.

| HOCl inhibition (%) | | | |
|---|---|---|---|
| Concentration (μg/mL) | FA | NP-PLGA-CS-FA | NP-B |
| 0 h | | | |
| 0.5 | $27 \pm 13^{a}$ | $15 \pm 9^{a}$ | $28 \pm 6^{a}$ |
| 1.0 | $61 \pm 7^{a}$ | $42 \pm 4^{b}$ | $28 \pm 12^{c}$ |
| 2.0 | $90 \pm 3^{a}$ | $32 \pm 8^{b}$ | $31 \pm 6^{b}$ |
| 2.5 | $93 \pm 2^{a}$ | $45 \pm 5^{b}$ | $27 \pm 11^{b}$ |
| 24 h | | | |
| 0.5 | $24 \pm 7^{a}$ | $26 \pm 8^{a}$ | $15 \pm 7^{a}$ |
| 1.0 | $68 \pm 10^{a}$ | $40 \pm 9^{b}$ | $17 \pm 9^{c}$ |
| 2.0 | $93 \pm 3^{a}$ | $54 \pm 12^{b}$ | $27 \pm 7^{c}$ |
| 2.5 | $94 \pm 5^{a}$ | $65 \pm 1^{b}$ | $29 \pm 13^{c}$ |
| 48 h | | | |
| 0.5 | $24 \pm 5^{a}$ | $25 \pm 8^{a}$ | $9 \pm 13^{a}$ |
| 1.0 | $33 \pm 7^{a,b}$ | $46 \pm 10^{a}$ | $10 \pm 13^{b}$ |
| 2.0 | $85 \pm 7^{a}$ | $51 \pm 8^{b}$ | $6 \pm 7^{c}$ |
| 2.5 | $97 \pm 1^{a}$ | $52 \pm 13^{b}$ | $12 \pm 10^{c}$ |
| 96 h | | | |
| 0.5 | $37 \pm 2^{a,b}$ | $21 \pm 11^{a}$ | $39 \pm 2^{b}$ |
| 1.0 | $67 \pm 13^{a}$ | $32 \pm 27^{b}$ | $26 \pm 11^{b}$ |
| 2.0 | $75 \pm 8^{a}$ | $33 \pm 12^{b}$ | $34 \pm 12^{b}$ |
| 2.5 | $89 \pm 1^{a}$ | $69 \pm 9^{a}$ | $29 \pm 9^{b}$ |

[a,b,c]Percent inhibition of hypochlorous acid ± standard deviation per line analysed. Same letters mean statistical equality and inequality statistics are shown for different letters (two-way ANOVA with post-Tukey test and $\alpha = 0.05$) ($n = 3$).

## Hypochlorous acid (HOCl) scavenging assay

Hypochlorous acid (HOCl) is a powerful oxidant produced by activated neutrophils. This acid is obtained from the myeloperoxidase catalysed reaction, in which the $H_2O_2$ reacts with chloride ions [27]. It is believed that HOCl is correlated with the defense against microorganisms, but its excess can be harmful, leading to tissue damage and diseases such as atherosclerosis and cancer [28]. The results of HOCl scavenging activity of free FA, NP-B and NP-PLGA-CS-FA were expressed as percentage of HOCl inhibition and are presented in Table 2. Significant differences were observed for the concentration factor, for the group factor (free FA, NP-PLGA-CS-FA and NP-B) and for the interaction between them, in all times analysed.

Free FA showed a concentration-dependent antioxidant activity. At 0 h, HOCl was inhibited using the highest concentration and the antioxidant activity was maintained during all the assay. This high antioxidant activity was expected, since FA has already been used in cosmetic products to retard and prevent cell aging and as a photoprotector [29]. Besides, many studies report its outstanding antioxidant properties, including their relation to anticarcinogenic and chemopreventive [30], antibacterial [31], antifungal [32] and neuroprotective effects [33,34]. The ability of FA to form a phenoxy radical stabilized by resonance is that allows its action and used as an antioxidant. Moreover, NP-B also presented a slight antioxidant activity during all experiment and it is probably due to CS coating of nanoparticles, since its antioxidant properties have been reported [3,35].

The results of HOCl inhibition by NP-PLGA-CS-FA show that until 48 h of assay, the antioxidant activity was lower than free FA ($p < .05$). This is due to the slow and sustained FA release, as demonstrated in the *in vitro* release assay. In 96 h of assay, in the highest sample concentration, the antioxidant activity of NP-PLGA-CS-FA was similar to that of free FA ($p > .05$). It may be assumed that the antioxidant activity achieved by NP-PLGA-CS-FA is a sum of the inhibitions caused by the FA released and by the CS present in nanoparticles. This phenomenon explains how a high inhibition of HOCl was obtained from NP-PLGA-CS-FA, whereas in the *in vitro* release profile in PBS only 25% of FA was released within 96 h.

The results show that FA encapsulation in PLGA nanoparticles coated with CS did not inhibit its high antioxidant activity. Moreover, the CS coating increased the potential use of the system as an antioxidant. In addition, the slow, cumulative and prolonged FA release in the medium decreases it metabolism prior to its pharmacological action. These characteristics, associated with pharmacokinetic advantages of nanoparticles, demonstrate that nanoparticles may have an even more promising antioxidant effect than free FA.

## Cytotoxicity assays

### Cytotoxicity over HeLa and B16-F10 tumour cells lines

One of the therapeutic properties of phenolic compounds, such as FA, is their antitumour activity, acting in the processes of initiation, promotion and progression of tumours [36]. FA, in particular, can inhibit the development of tumours by capturing ROS, or for its involvement in the cell cycle by cellular uptake [37]. In this study, the determination of the cytotoxic activity of free FA, NP-PLGA-CS-FA and NP-B over B16-F10 and HeLa tumour cells was evaluated for a period of 48 h. Furthermore, tests with solvents were also performed, and these showed, at all times, cell viabilities around 100%, confirming their non-interference in the obtained data. The results were expressed as a percentage of cell viability and are presented in Figure 3.

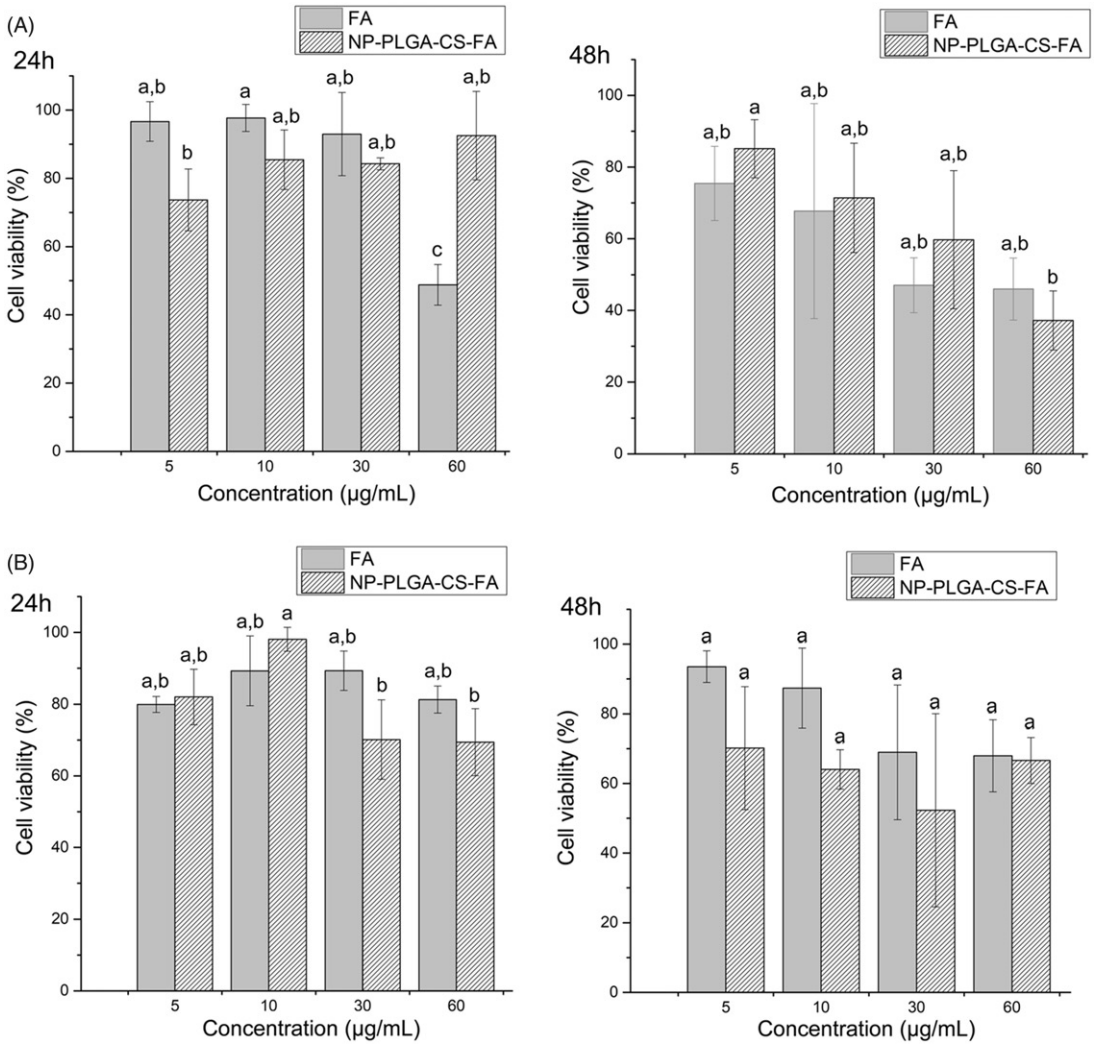


**Figure 3.** Effect of free ferulic acid (FA) and PLGA-CS-FA nanoparticles on the viability of (A) B16-F10 and (B) HeLa cell lines. Results were expressed as mean ± standard deviation ($n = 3$). (a, b, c) Data analysed by concentration. Same letters mean equality statistics and different letters inequality statistics (Two-way ANOVA with post-Tukey test and $\alpha < 0.05$).

At 24 h period, for the assays with B16-F10 cell line, in the concentrations of 5, 10 and 30 μg/mL, there was no statistical difference ($p > .05$) between the antitumour activity obtained by the free FA and the NP-PLGA-CS-FA. Moreover, this activity was very discreet, exhibiting a minimum cellular viability of 74%. However, at the concentration of 60 μg/mL, free FA presented higher activity than NP-PLGA-CS-FA, since their cellular viabilities were 49% and 93%, respectively. It can be due to the slow FA release rate from nanoparticles, as evidenced by the *in vitro* release assay, in which only 20% of the encapsulated FA was released into the medium within 24 h. For the test performed with HeLa tumour cells, there was no significant difference ($p > .05$) between the cell viability obtained by FA and FA-loaded nanoparticles, at all tested concentrations.

At 48 h, the inhibitions of both B16-F10 and HeLa cells were increased, and for all concentrations there was no significant difference ($p > .05$) between FA in solution and NP-PLGA-CS-FA. The concentration factor presented differences for the B16-F10 cell line ($p < .05$) and absence of significant differences for the HeLa cell line ($p > .05$). For the B16-F10 cell line, the lowest viability occurred at the concentration of 60 μg/mL, being 46% for free FA and 37% for FA nanoparticles. While for HeLa cells, the antitumour activity was lower, suggesting that the action of FA over B16-F10 cells is more effective. The cell viability of HeLa cells reached a minimum of 52% using a concentration of 30 μg/mL for the NP-PLGA-CS-FA. The results presented in the tests with both tumour cell lines were promising, since they demonstrate that the nanoencapsulation of FA did not inhibit the antitumour activity of FA.

Moreover, at 24 and 48 h, NP-B presented a cell viability between 70 and 80% for B16-F10 cells and 75 and 60% for HeLa (data not shown), indicating that the nanoparticles *per se* exert some cytotoxic activity. For this reason, although the FA release from the nanoparticles occurs in a slow and prolonged way, the cellular inhibition was similar to that achieved by the isolated drug in the short period of 48 h, since the antitumour activity of the nanoparticles does not come only from the drug, but also from the carrier system. The cytotoxic activity of nanoparticles without FA maybe possibly due to the presence of CS [38–40]. It is reported that the antitumour activity of CS is due to inductive activities of apoptosis and membrane rupture [39].

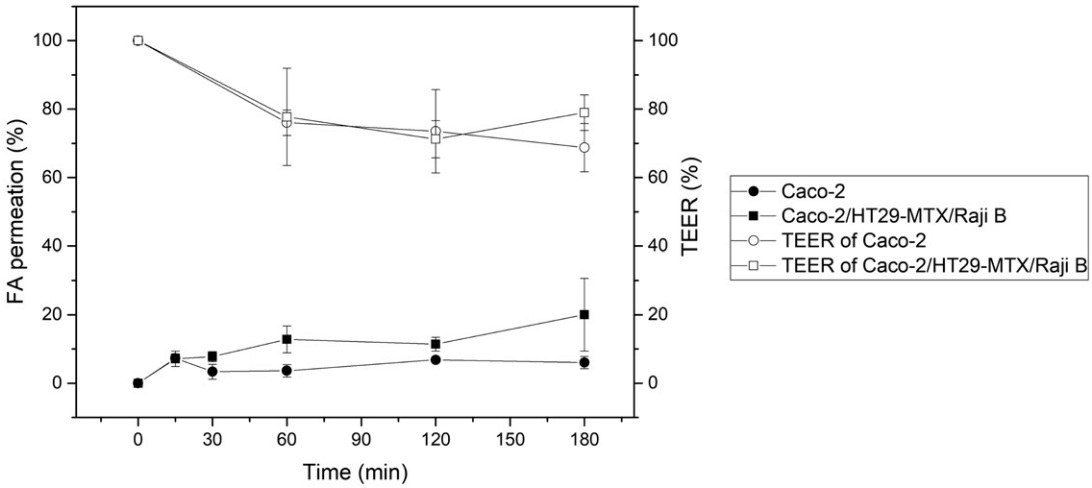


**Figure 4.** Cumulative ferulic acid (FA) permeation and TEER cell monolayer measurements across monolayers of Caco-2 and Caco-2/HT29-MTX/Raji B triple co-culture. Results were expressed as mean ± standard deviation ($n = 3$).

We can hypothesize that the *in vivo* application of NP-PLGA-CS-FA can bring different and potentially higher results, since nanoparticles improve the biopharmaceutical and pharmacokinetic parameters faced by the FA, increasing its half-life time and consequently its bioavailability. The encapsulation of antitumour drugs can also lead to a tumour-specific release, increasing the permeability and retention of these agents due to the Enhanced Permeability and Retention Effect (EPR).

## *In vitro* intestinal permeability assay

In order to select drugs and evaluate their intestinal absorption potential, many *in vitro* models have been studied and used [41]. These models present advantages when compared to the *in vivo* tests of intestinal permeability, since besides being less laborious and with lower costs, they also present benefits on ethical issues [42]. In this assay, the assessment of intestinal permeability of NP-PLGA-CS-FA was performed and compared in two different cell models, Caco-2 cell monolayer and triple co-culture of Caco-2/HT29-MTX/Raji B cell monolayer. This last intestinal monolayer model is more similar to *in vivo* conditions than Caco-2 cell monolayer, as it presents enterocytes (Caco-2 cells), the mucus-producing goblet cells (HT29-MTX) in physiological proportions (90:10) and the induction of M cells by Raji B [13,43,44].

Figure 4 shows the cumulative amount of permeated FA from nanoparticles and the TEER values obtained, both expressed as percentage, for the Caco-2 monolayer and for the triple co-culture of Caco-2/HT29-MTX/Raji B. The FA permeation reached a maximum of 20% through the triple co-culture and 5% through Caco-2 cells. This result is due to the slow and sustained release of FA from the NP-PLGA-CS, since according to *in vitro* release assay about 17% of FA was released in PBS within 180 min. Araújo et al. [13] also obtained a lower permeability of GLP-1 when it was encapsulated in nanoparticles composed of PLGA, Witepsol E85 lipid or porous silicone, and authors related this fact to the sustained drug release pattern from these nanoparticles. It was also observed that the permeability of the encapsulated FA was higher in the triple co-culture model than in the monolayer Caco-2 model ($p < .05$). The presence of mucus produced by HT29-MTX cells, composed largely of negatively charged glycoproteins [45], is mainly responsible for this increased permeability. The CS present in the coating of the nanoparticles, due to its positively charged surface, presents mucoadhesive properties, allowing a greater contact of the nanoparticles with the intestinal epithelium [13,17,43–46]. Thus, there is an increase in drug concentration at the site of absorption and a higher para- or transcellular permeation of it. In addition, the presence of M cells in the Caco-2/HT29-MTX/Raji B triple co-culture model, may also enable an increase in cell permeability, since these cells are specialized in the uptake of microorganisms and antigens, and can act as a gateway for intestinal absorption of proteins and nanoparticles [13,43].

Regarding TEER values, a slight decrease in the values was observed before and after the permeability test, reaching a minimum of 31% below the initial value, a result of the opening of cellular tight junctions [47]. However, there was no significant difference ($p > .05$) between TEER percentages obtained for the free and encapsulated FA and between the two models, thus demonstrating the similar integrity of the cell monolayers.

## Conclusions

NP-PLGA-CS-FA were efficiently obtained by the single-emulsion solvent evaporation technique and presented suitable physicochemical characteristics for the transport of FA. The mean diameter was below 300 nm, and the zeta potential presented positive and far from neutrality, due to the presence of CS in the coating of the particles. The encapsulation process allowed the sustained release of this compound, being this release regulated by the diffusion process. The antioxidant and cytotoxic activities of FA were confirmed and maintained after its encapsulation, being these activities possibly the result of combined action of FA and CS. Moreover, the nanoparticles maintained their stability in simulated gastric and intestinal fluids, demonstrating resistance to the pH

changes and avoiding the premature FA release. And finally, the intestinal permeability of NP-PLGA-CS-FA was more prominent in the presence of mucus and M cells, mainly due to the presence of the mucoadhesive CS-coating. Thus, the developed PLGA-CS nanoparticles are shown to be promising carriers for the controlled release of FA from oral administration.

## Disclosure statement

No potential conflict of interest was reported by the authors.

## Funding

This study was supported by the CAPES (Coordenação de Aperfeiçoamento de Pessoal de Nível Superior) in the form of doctoral fellowship for I.A. de Lima, Fundação Araucária (17/17) CNPq (Conselho Nacional de Desenvolvimento Científico e tecnológico) and Finep (Financiadora de Estudos and Projetos) for partial financial support.

## ORCID

Najeh Maissar Khalil http://orcid.org/0000-0002-5140-9944
Anna Lechanteur http://orcid.org/0000-0001-6586-8896
Bruno Sarmento http://orcid.org/0000-0001-5763-7553
Rubiana Mara Mainardes http://orcid.org/0000-0002-4442-2075

## References

[1] Mancuso C, Santangelo R. Ferulic acid: pharmacological and toxicological aspects. Food Chem Toxicol. 2014;65:185–195.
[2] Kumar N, Pruthi V. Potential applications of ferulic acid from natural sources. Biotechnol Rep (Amst). 2014;4:86–93.
[3] Ngo DH, Kim SK. Antioxidant effects of chitin, chitosan, and their derivatives. Adv Food Nutr Res. 2014;73:15–31.
[4] Liu J, Wen XY, Lu JF, et al. Free radical mediated grafting of chitosan with caffeic and ferulic acids: structures and antioxidant activity. Int J Biol Macromol. 2014;65:97–106.
[5] Zhang Y, Li Z, Zhang K, et al. Ethyl oleate-containing nanostructured lipid carriers improve oral bioavailability of trans-ferulic acid as compared with conventional solid lipid nanoparticles. Int J Pharm. 2016;511:57–64.
[6] Li C, Li JB. Preparation of chitosan-ferulic acid conjugate: structure characterization and in the application of pharmaceuticals. Int J Biol Macromol. 2017;105:1539–1543.
[7] Dong GC, Kuan CY, Subramaniam S, et al. A potent inhibition of oxidative stress induced gene expression in neural cells by sustained ferulic acid release from chitosan based hydrogel. Mater Sci Eng C. 2015;49:691–699.
[8] Bhathena J, Toamro-Duchesneau C, Martoni C, et al. Effect of orally administered microencapsulated FA-producing *L. fermentum* on markers of metabolic syndrome: an in vivo analysis. J Diabetes Metab. 2012;S6:006.
[9] Chaves LL, Costa Lima SA, Vieira ACC, et al. Development of PLGA nanoparticles loaded with clofazimine for oral delivery: assessment of formulation variables and intestinal permeability. Eur J Pharm Sci. 2018;112:28–37.
[10] Mir M, Ahmed N, Rehman AU. Recent applications of PLGA based nanostructures in drug delivery. Colloids Surf B Biointerfaces. 2017;159:217–231.
[11] Wei Z, Wang C, Zou S, et al. Chitosan nanoparticles as particular emulsifier for preparation of novel pH-responsive Pickering emulsions and PLGA microcapsules. Polymer. 2012;53:1229–1235.
[12] Chronopoulou L, Massimi M, Giardi MF, et al. Chitosan-coated PLGA nanoparticles: a sustained drug release strategy for cell cultures. Colloids Surf B Biointerfaces. 2013;103:310–317.
[13] Araújo F, Shrestha N, Shahbazi MA, et al. The impact of nanoparticles on the mucosal translocation and transport of GLP-1 across the intestinal epithelium. Biomaterials. 2014;35:9199–9207.
[14] Ludwig DB, de Camargo LEA, Khalil NM, et al. Antifungal activity of chitosan-coated poly(lactic-co-glycolic) acid nanoparticles containing amphotericin B. Mycophatologia. 2018. DOI: 10.1007/s11046-018-0253-x
[15] Lima IA, Khalil NM, Mainardes RM. A stability-indicating HPLC-PDA method for the determination of ferulic acid in chitosan-coated poly(lactide-co-glycolide) nanoparticles. Braz J Pharm Sci. 2017;53:e16138.
[16] Ritger PL, Peppas NA. A simple equation for description of solute release II. Fickian and anomalous release from swellable devices. J Control Release. 1987;5:37–42.
[17] Antunes F, Andrade F, Araújo F, et al. Establishment of a triple co-culture in vitro cell models to study intestinal absorption of peptide drugs. Eur J Pharm Biopharm. 2013;83:427–435.
[18] Araújo F, Sarmento B. Towards the characterization of an in vitro triple co-culture intestine cell model for permeability studies. Int J Pharm. 2013;458:128–134.
[19] Guo C, Gemeinhart RA. Understanding the adsorption mechanism of chitosan onto poly(lactide-co-glycolide) particles. Eur J Pharm Biopharm. 2008;70:597–604.
[20] Nafee N, Schneider M, Schaefer UF, et al. Relevance of the colloidal stability of chitosan/PLGA nanoparticles on their cytotoxicity profile. Int J Pharm. 2009;381:130–139.
[21] Yuan X, Shah BA, Kotadia NK, et al. The development and mechanism studies of cationic chitosan-modified biodegradable PLGA nanoparticles for efficient siRNA drug delivery. Pharm Res. 2010;27:1285–1295.
[22.] Gupta RB. Fundamentals of drug nanoparticles. In: Gupta RB, Kompella UB, editors. Nanoparticle technology for drug delivery. New York (NY): Taylor & Francis Group; 2006. p. 1–18.
[23] Sahoo SK, Labhasetwar V. Nanoparticle interface: an important determinant in nanoparticle-mediated drug/gene delivery. In: Gupta RB, Kompella UB, editors. Nanoparticle technology for drug delivery. New York (NY): Taylor & Francis Group; 2006. p. 139–154.
[24] Wang Y, Li P, Kong L. Chitosan-modified PLGA nanoparticles with versatile surface for improved drug delivery. AAPS PharmSciTech. 2013;14:585–592.
[25] Parveen S, Sahoo SK. Long circulating chitosan/PEG blended PLGA nanoparticle for tumor drug delivery. Eur J Pharmacol. 2011;670:372–383.
[26] Xiong XY, Tam KC, Gan LH. Release kinetics of hydrophobic and hydrophilic model drugs from pluronic F127/poly(lactic acid) nanoparticles. J Control Release. 2005;103:73–82.
[27] Gatto MT, Firuzi O, Agostino R, et al. Development of a new assay for the screening of hypochlorous acid scavengers based on reversed-phase high-performance liquid chromatography. Biomed Chromatogr. 2002;16:404–411.
[28] Miyamoto S, Martinez GR, Rettori D, et al. Linoleic acid hydroperoxide reacts with hypochlorous acid, generating peroxyl radical intermediates and singlet molecular oxygen. Proc Natl Acad Sci USA. 2006;103:293–298.
[29] Saija A, Tomaino A, Cascio RL, et al. Ferulic and caffeic acids as potential protective agents against photooxidative skin damage. J Sci Food Agric. 1999;79:476–480.
[30] Jayaprakasam B, Vanisree M, Zhang Y, et al. Impact of alkyl esters of caffeic and ferulic acids on tumor cell proliferation, cyclooxygenase enzyme, and lipid peroxidation. J Agric Food Chem. 2006;54:5375–5381.
[31] Lee DS, Woo JY, Ahn CB, et al. Chitosan-hydroxycinnamic acid conjugates: preparation, antioxidant and antimicrobial activity. Food Chem. 2014;148:97–104.
[32] Panwar R, Pemmaraju SC, Sharma AK, et al. Efficacy of ferulic acid encapsulated chitosan nanoparticles against *Candida albicans* biofilm. Microb Pathog. 2016;95:21–31.

[33] Cheng CY, Su SY, Tang NY, et al. Ferulic acid provides neuroprotection against oxidative stress-related apoptosis after cerebral ischemia/reperfusion injury by inhibiting ICAM-1 mRNA expression in rats. Brain Res. 2008;1209:136–150.

[34] Koh PO. Ferulic acid prevents the cerebral ischemic injury-induced decrease of Akt and Bad phosphorylation. Neurosci Lett. 2012; 507:156–160.

[35] Kerch G. The potential of chitosan and its derivatives in prevention and treatment of age-related diseases. Mar Drugs. 2015;13: 2158–2182.

[36] Dai J, Mumper RJ. Plant phenolics: extraction, analysis and their antioxidant and anticancer properties. Molecules. 2010;15: 7313–7352.

[37] Yang GW, Jiang JS, Lu WQ. Ferulic acid exerts anti-angiogenic and anti-tumor activity by targeting fibroblast growth factor receptor 1-mediated angiogenesis. Int J Mol Sci. 2015;16:24011–24031.

[38] Qi LF, Xu ZR, Li Y, et al. In vitro effects of chitosan nanoparticles on proliferation of human gastric carcinoma cell line MGC803 cells. World J Gastroenterol. 2005;11:5136–5141.

[39] Qi L, Xu Z. In vivo antitumor activity of chitosan nanoparticles. Bioorg Med Chem Lett. 2006;16:4243–4245.

[40] Qin C, Du Y, Xiao L, et al. Enzymic preparation of water-soluble chitosan and their antitumor activity. Int J Biol Macromol. 2002; 31:111–117.

[41] Lechanteur A, das Neves J, Sarmento B. The role of mucus in cell-based models used to screen mucosal drug delivery. Adv Drug Deliv Rev. 2017;124:50–63.

[42] Jain AS, Dhawan VV, Sarmento B, et al. In vitro and ex vivo evaluations of lipid anti-cancer nanoformulations: insights and assessment of bioavailability enhancement. AAPS PharmSciTech. 2016; 17:553–571.

[43] Shrestha N, Shahbazi M-A, Araújo F, et al. Multistage pH-responsive mucoadhesive nanocarriers prepared by aerosol flow reactor technology: a controlled dual protein-drug delivery system. Biomaterials. 2015;68:9–20.

[44] Lopes M, Shrestha N, Correia A, et al. Dual chitosan/albumin-coated alginate/dextran sulfate nanoparticles for enhanced oral delivery of insulin. J Control Release. 2016;232:29–41.

[45] Madureira AR, Campos DA, Oliveira A, et al. Insights into the protective role of solid lipid nanoparticles on rosmarinic acid bioactivity during exposure to simulated gastrointestinal conditions. Colloids Surf B Biointerfaces. 2016;139:277–284.

[46] Shrestha N, Shahbazi MA, Araújo F, et al. Chitosan-modified porous silicon microparticles for enhanced permeability of insulin across intestinal cell monolayers. Biomaterials. 2014;35:7172–7179.

[47] Silva DS, Almeida A, Prezotti F, et al. Synthesis and characterization of 3,6-O,O'-dimyristoyl chitosan micelles for oral delivery of paclitaxel. Colloids Surf B Biointerfaces. 2017;152:220–228.